REGULAR ARTICLE

blood advances

Analysis of MCFD2- and LMAN1-deficient mice demonstrates distinct functions in vivo

Min Zhu,[1,2,*] Chunlei Zheng,[1,*] Wei Wei,[1] Lesley Everett,[3] David Ginsburg,[3-7] and Bin Zhang[1]

[1]Genomic Medicine Institute, Lerner Research Institute of Cleveland Clinic, Cleveland, OH; [2]Department of Pathology, Karamay Central Hospital, Karamay, China; and [3]Life Sciences Institute, [4]Department of Internal Medicine, [5]Department of Human Genetics, [6]Department of Pediatrics and Communicable Diseases, and [7]Howard Hughes Medical Institute, University of Michigan, Ann Arbor, MI

Key Points

- LMAN1 and MCFD2 have distinct functions and are required for ER-to-Golgi transport of FV, FVIII, and α1-antitrypsin.
- An alternative transport pathway is responsible for remaining FV/FVIII secretion in LMAN1/MCFD2-deficient mice.

The LMAN1–MCFD2 complex serves as a cargo receptor for efficient transport of factor V (FV) and FVIII from the endoplasmic reticulum (ER) to the Golgi. Genetic deficiency of *LMAN1* or *MCFD2* in humans results in the moderate bleeding disorder combined FV and FVIII deficiency, with a similar phenotype previously observed in LMAN1-deficient mice. We now report that MCFD2-deficient mice generated by gene targeting also demonstrate reduced plasma FV and FVIII, with levels lower than those in LMAN1-deficient mice, similar to previous observations in LMAN1- and MCDF2-deficient humans. Surprisingly, FV and FVIII levels in doubly deficient mice match the higher levels observed in LMAN1-deficient mice. In contrast to the strain-specific partial lethality previously observed in LMAN1-null mice, MCFD2-null mice demonstrate normal survival in different genetic backgrounds, although doubly deficient mice exhibit partial embryonic lethality comparable to LMAN1-deficient mice. These results suggest that an alternative pathway is responsible for FV/FVIII secretion in doubly deficient mice and distinct cargo-specific functions for LMAN1 and MCFD2 within the ER-to-Golgi secretory pathway. We also observed decreased plasma levels of α1-antitrypsin (AAT) in male mice for all 3 groups of deficient mice. Comparable accumulation of AAT was observed in hepatocyte ER of singly and doubly deficient mice, demonstrating a role for LMAN1 and MCFD2 in efficient ER exit of AAT.

Introduction

Coagulation factor V (FV) and FVIII are large plasma glycoproteins that share similar domain structures and play pivotal roles in hemostasis and thrombosis.[1] Activated FV and FVIII serve as nonenzymatic cofactors for FXa and FIXa, respectively, with mutations in FV resulting in inherited FV deficiency and mutations in FVIII resulting in hemophilia A. Combined deficiency of FV and FVIII (F5F8D) is an autosomal recessive bleeding disorder that is characterized by simultaneous reduction of both cofactors[2,3] resulting from loss-of-function mutations in *LMAN1* or *MCFD2*.[4,5] LMAN1 is a transmembrane lectin that contains a carbohydrate binding domain localized to the endoplasmic reticulum (ER) lumen, as well as cytoplasmic motifs for ER exit and retrieval.[6-8] MCFD2 is a small soluble protein with 2 EF-hand domains at the C terminus and an unstructured sequence at the N terminus.[5,9,10] The carbohydrate-recognition domain of LMAN1 and the EF-hand domains of MCFD2 interact to form a Ca^{2+}-dependent protein complex that cycles between the ER and the ER–Golgi intermediate compartment (ERGIC), an organelle that is unique to higher eukaryotic cells.

Submitted 5 March 2018; accepted 14 April 2018. DOI 10.1182/bloodadvances.2018018317.

*M.Z and C.Z. contributed equally to this work.

The LMAN1–MCFD2 complex is thought to function as a cargo receptor required for efficient secretion of FV and FVIII.[5,11,12] Cargo receptors capture and concentrate specific cargo proteins into COPII-coated vesicles in the ER.[13,14] After budding, these vesicles fuse to form the ERGIC, where cargo proteins are separated from the cargo receptor and continue their journey through the secretory pathway. The dissociation of FV/FVIII from the LMAN1–MCFD2 complex may be triggered by a drop in Ca^{2+} concentration in the ERGIC.[15] Cargo receptors are recycled to the ER via COPI-coated vesicles for additional rounds of cargo transport. LMAN1 and MCFD2 interact with FV/FVIII, suggesting distinct and essential roles for both subunits of the protein complex in FV/FVIII transport.[10-12] LMAN1–MCFD2 is the first known example of a specific ER-to-Golgi cargo receptor in vertebrates, with the requirement for a transmembrane component (LMAN1) and a soluble cofactor (MCFD2) suggesting a more complex trafficking mechanism than previously characterized cargo receptors in yeast.

Residual FV and FVIII secretion in subjects with *LMAN1* or *MCFD2* mutations results in plasma levels of 5-30% compared with normal controls, although the range of levels observed in MCFD2-deficient subjects is slightly lower than in subjects with *LMAN1* mutations.[16] Previously, we reported that LMAN1-deficient mice exhibit a strain-specific partial lethal phenotype, decreased levels of plasma FV and FVIII, and decreased platelet FV, although both are more moderately reduced than in humans.[17,18] Hepatocytes of LMAN1-deficient mice also accumulate α1-antitrypsin (AAT), an inhibitor of neutrophil elastase and an acute-phase reactant[19] previously identified as a potential cargo of LMAN1.[20] Studies of conditional LMAN1-knockout (KO) mice demonstrate that FVIII is exclusively synthesized in endothelial cells.[18] We now report the characterization of gene-targeted mice deficient in MCFD2, demonstrating a further reduction in plasma FV and FVIII levels compared with LMAN1-deficient mice as in humans, as well as a defect in AAT secretion, with doubly deficient mice exhibiting higher FV and FVIII levels comparable to LMAN1-deficient mice.

Methods

MCFD2 gene targeting

We designed a targeting vector in pCKO[21] that would replace exons 2 and 3 of the murine *Mcfd2* gene with a neomycin expression cassette. This vector was electroporated into 129/svImJ mouse embryonic stem (ES) cells. ES cell clones were initially screened using a TaqMan-based polymerase chain reaction (PCR) method,[22] which identified 1 clone with homologous recombination that results in reduction to only a single copy of the wild-type (WT) *Mcfd2* allele. After further confirmation by Southern blot analysis (Figure 1), ES cells were expanded and injected into blastocysts derived from C57BL/6J mice by the Transgenic Mouse Core at the University of Michigan, which were then implanted into pseudo-pregnant female mice. The resulting male chimeric offspring were mated with female C57BL/6J or 129/svImJ mice to generate F1 mice with germline transmission. MCFD2-deficient mice were also crossed with previously reported LMAN1-deficient mice with a gene-trap allele (*gt1*)[17] to generate offspring with double deficiencies. All mice had free access to food and water and were kept in cages in a 12-hour light/dark cycle. All animal experimental protocols were approved by the Institutional Animal Care and Use Committees at the University of Michigan and the Cleveland Clinic.

Genotyping

Genotyping was carried out by a 3-primer PCR assay of genomic DNA prepared from tail clippings of pups. Primers flanking the 3′ end of the left arm within intron 1 of *Mcfd2* (L1, AGGAGAG-CAAGCCAATTCTG; L2, TGAAAACCCCTCACTCTGCT) were combined with a primer located in the vector sequence inserted into the genome (V1, CTAAAGCGCATGCTCCAGAC) to generate different-sized PCR products from the WT (201 bp) and the targeted allele (248 bp) (Figure 1).

Measurement of FV and FVIII levels

Mouse plasma was collected as previously described.[17] We developed a murine FV-specific enzyme-linked immunosorbent assay (ELISA) using 2 monoclonal anti-murine FV antibodies from Green Mountain Antibodies (Burlington, VT). Clone GMA-752 was used as a capture antibody, and biotinylated clone GMA-754 was used as a detection antibody. Previously tested antibodies were unable to detect intracellular FV in mouse liver.[17,23,24] Clone GMA-753 was found to detect intracellular FV in mouse liver extracts by western blot analysis. FVIII activity was measured using a chromogenic assay kit (Chromagenix, Milano, Italy) that detects human and murine FVIII.[25] Pooled WT mouse plasma was used as a standard. Measurements of FV and FVIII were carried out on 3 different days with 3 different batches of plasma samples, with each batch containing all 4 genotypes (WT, LMAN1-deficient, MCFD2-deficient, and doubly deficient mice).

Measurement of AAT levels

Mouse plasma AAT levels were measured using an ELISA kit (ICL Laboratory, Portland, OR). Western blot analysis of intracellular and secreted AAT was performed using a rabbit anti-AAT (Antibodies-online, Atlanta, GA).

Immunofluorescence imaging

WT, $Lman1^{gt1/gt1}$, $Mcfd2^{-/-}$, and $Lman1^{gt1/gt1}Mcfd2^{-/-}$ mouse liver sections were embedded in Tissue-Tek optimal cutting temperature compound (Sakura Finetek, Torrance, CA), as previously described.[26,27] Cryosections (6 μm) were permeabilized with 0.1% Triton X-100 and incubated with chicken anti-mouse AAT (ICL Laboratory), followed by an Alexa Fluor 488–conjugated secondary antibody (Thermo Fisher, Waltham, MA). Cover slips were mounted using mounting medium (Vector Laboratories, Burlingame, CA), and images were captured using an Olympus FluoView confocal microscope.

Statistical analysis

A 2-tailed Student *t* test was used to assess the significance of differences between 2 groups of data. The χ^2 test was used to evaluate the significance of differences between the expected and observed genotype distributions. To investigate whether doubly deficient mice were unrepresented, we used logistic regression to compute the odds ratio (OR) and confidence intervals (CIs) between observations and expectations.

Results

Generation of MCFD2-deficient mice

The targeting construct was designed to delete exons 2 and 3 of *Mcfd2* (Figure 1A), which contain the majority of the coding

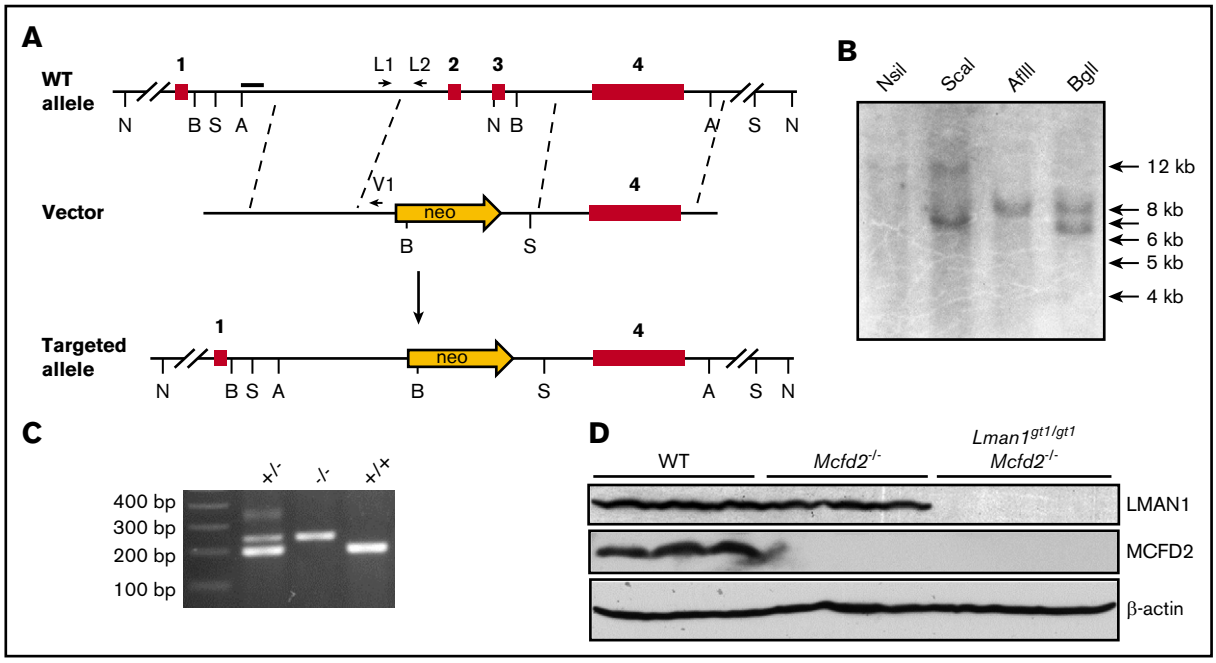

Figure 1. Generation of mice with disruption of the *Mcfd2* allele. (A) Schematic diagram of the *Mcfd2* allele–targeting strategy. Locations of restriction enzymes, Southern blot probe, and genotyping primers are indicated. (B) Southern blot analysis of a targeted ES cell clone. Expected sizes of restriction fragments are (WT and KO) *Nsi*I, 12.7 and 19.2 kb; *Sca*I, 12.5 and 7.4 kb; *Afl*II, 9 and 8.5 kb; and *Bgl*II, 8.7 and 7.1 kb. Arrows indicate DNA ladder bands (kb). (C) Three-primer PCR genotyping results. The higher band in the heterozygous sample represents heteroduplex DNA. (D) Western blot analysis of liver lysates of WT, $Mcfd2^{-/-}$, and $Lman1^{gt1/gt1}/Mcfd2^{-/-}$ mice. Three individual mice from each genotype were analyzed. A, *Afl*II; B, *Bgl*II; N, *Nsi*I; S, *Sca*I.

sequence. Southern blot analysis confirmed correct integration of the targeting vector into the *Mcfd2* locus of the ES cell clone (Figure 1B). Mating of male chimeric mice with female C57BL/6J mice generated pups with germline transmission of the *Mcfd2* deletion allele that should be F1 for the C57BL/6J and 129/svlmJ genetic background, whereas mating of male chimeric mice to female 129/svlmJ mice generated pups with germline transmission of the *Mcfd2* deletion allele on the pure 129/svlmJ background. Intercrosses of F1 mice generated homozygote F2 mice (Figure 1C). Western blot analysis confirmed the absence of MCFD2 protein expression in $Mcfd2^{-/-}$ mice (Figure 1D). F1 C57BL/6J/129/svlmJ $Mcfd2^{+/-}$ mice were further backcrossed onto the C57BL/6J background for >10 generations.

Viability of MCFD2-deficient and LMAN1/MCFD2 double-deficient mice

We performed intercrosses of $Mcfd2^{+/-}$ mice backcrossed onto the C57BL/6 background for >10 generations, as well as $Mcfd2^{+/-}$ mice on the 129/svlmJ background and the mixed C57BL/6 and 129/svlmJ genetic background (F1 and F2 mice). The expected Mendelian ratio of genotypes was observed in the offspring of all intercrosses at weaning (Table 1), indicating that MCFD2 is not required for murine development or survival. No spontaneous bleeding was observed in $Mcfd2^{-/-}$ mice, and bleeding time from tail vein transection[28,29] was indistinguishable between $Mcfd2^{-/-}$ mice (62 ± 24 seconds, n = 14) and WT controls (57 ± 17 seconds, n = 11) on the C57BL/6 background, consistent with a previous report using $Lman1^{-/-}$ mice.[17] Previously reported LMAN1-deficient mice with a gene-trap allele (*gt1*)[17] that had been backcrossed with C57BL/6J mice for >16 generations were mated with $Mcfd2^{+/-}$ mice on the 129/svlmJ background to produce double-heterozygous mice on a mixed C57BL/6 and 129/svlmJ genetic background or with $Mcfd2^{+/-}$ mice backcrossed with C57BL/6J mice for 10 generations to produce double-heterozygous mice on the C57BL/6J background. To assess the viability of LMAN1/MCFD2 double-KO (DKO) mice, we first performed intercrosses of $Lman1^{+/gt1}Mcfd2^{+/-}$ mice on a mixed C57BL/6 and 129/svlmJ genetic background (Table 2). Western blot analysis confirmed the absence of LMAN1 and MCFD2 in $Lman1^{gt1/gt1}Mcfd2^{-/-}$ mice (Figure 1D). No significant decrease in the number of $Lman1^{gt1/gt1}Mcfd2^{-/-}$ mice was observed (P = .670; OR, 0.82; 95% CI, 0.34-1.95).

Table 1. Genotype distributions for progeny of an $Mcfd2^{+/-}$ intercross on different genetic backgrounds

Expected	+/+ (25%)	+/− (50%)	−/− (25%)	*P**
Observed on mixed background (n = 199), % (n)	20.10 (40)	54.27 (108)	25.63 (51)	>0.26
Observed on C57BL/6J (n = 73), % (n)	27.40 (20)	47.95 (35)	24.66 (18)	>0.89
Observed on 129/svlmJ (n = 64), % (n)	28.13 (18)	50.00 (32)	21.88 (14)	>0.77

*χ^2 results between expected genotype distribution and observed genotype distribution.

Table 2. Genotype distributions of intercrosses between double heterozygous mice and crosses between *Mcfd2*$^{-/-}$*Lman1*$^{+/gt1}$ and *Mcfd2*$^{+/-}$*Lman1*$^{+/gt1}$ mice

Crosses	Genotype distribution									P
***Mcfd2*$^{+/-}$*Lman1*$^{+/gt1}$ × *Mcfd2*$^{+/-}$*Lman1*$^{+/gt1}$**	$M^{-/-},L^{gt1/gt1}$	$M^{+/-},L^{gt1/gt1}$	$M^{+/+},L^{gt1/gt1}$	$M^{+/-},L^{+/gt1}$	$M^{+/+},L^{+/gt1}$	$M^{-/-},L^{+/+}$	$M^{+/-},L^{+/+}$	$M^{+/+},L^{+/+}$		
Expected, %	6.25	12.5	6.25	12.5	25	12.5	6.25	12.5	6.25	
Observed on mixed background (n = 184), % (n)	5.43 (10)	10.33 (19)	5.43 (10)	14.13 (26)	27.17 (50)	10.33 (19)	5.43 (10)	15.76 (29)	5.98 (11)	0.67
Observed on C57BL/6J (n = 343), % (n)	2.62 (9)	8.16 (28)	3.21 (11)	16.91 (58)	26.82 (92)	12.83 (44)	7.00 (24)	16.91 (58)	5.54 (19)	0.028
***Mcfd2*$^{-/-}$*Lman1*$^{+/gt1}$ × *Mcfd2*$^{+/-}$*Lman1*$^{+/gt1}$**	$M^{-/-},L^{gt1/gt1}$	$M^{+/-},L^{gt1/gt1}$	$M^{-/-},L^{+/gt1}$	$M^{+/-},L^{+/gt1}$	$M^{-/-},L^{+/+}$	$M^{+/-},L^{+/+}$				
Expected, %	12.5	12.5	25	25	12.5	12.5				
Observed on C57BL/6J (n = 342), % (n)	5.85 (20)	9.06 (31)	28.65 (98)	22.81 (78)	14.91 (51)	18.71 (64)				0.004

P values were calculated for *Mcfd2*$^{-/-}$ *Lman1*$^{gt1/gt1}$ mice vs all other genotypes using logistic regression.
L, *Lman1*; *M*, *Mcfd2*.

Next, we performed intercrosses of *Lman1*$^{+/gt1}$*Mcfd2*$^{+/-}$ mice on the C57BL/6 background (Table 2). We observed ~42% of the expected number of *Lman1*$^{gt1/gt1}$*Mcfd2*$^{-/-}$ mice ($P = .028$; OR, 0.41; 95% CI, 0.18-0.88), suggesting a partial lethal phenotype of DKO mice on this genetic background. In this mating, the *Lman1*$^{gt1/gt1}$ genotype (14.0%, $P < .001$) is underrepresented, whereas the *Mcfd2*$^{-/-}$ genotype (26.5%, $P > .7$) is of the expected number, suggesting that the partial lethal phenotype of DKO mice can be attributed to the *Lman1*$^{gt1/gt1}$ genotype. We also performed an *Lman1*$^{+/gt1}$*Mcfd2*$^{-/-}$ × *Lman1*$^{+/gt1}$*Mcfd2*$^{+/-}$ cross using the offspring of intercrosses of *Lman1*$^{+/gt1}$*Mcfd2*$^{+/-}$ mice and again observed a lower than expected number of DKO mice ($P = .004$; OR, 0.43; 95% CI, 0.24-0.74) and underrepresentation of the *Lman1*$^{gt1/gt1}$ genotype (14.9%; $P < .001$), with expected numbers for the *Mcfd2*$^{-/-}$ genotype (48%, $P > .8$). MCFD2-KO and surviving DKO mice exhibit normal growth, fertility, and gross appearance; no apparent abnormalities on standard necropsy evaluation; and normal overall survival (up to 1.5 years of follow-up).

FV, FVIII, and AAT levels in mice with single and double KO of LMAN1 and MCFD2

Mice were generated from intercrosses of *Lman1*$^{+/gt1}$*Mcfd2*$^{+/-}$ mice on the C57BL/6 background and intercrosses of the resulting offspring. Mean FV and FVIII levels in LMAN1-KO mice were decreased to 58% and 54% of WT levels, respectively ($P < .001$; Figure 2A), consistent with previous reports.[17] Average FV and FVIII levels in MCFD2-KO mice were further decreased to 35% and 33% of WT levels ($P < .0001$ for FV and $P < .005$ for FVIII between *Lman1*$^{gt1/gt1}$ and *Mcfd2*$^{-/-}$ mice). Surprisingly, average FV and FVIII levels in DKO mice are similar to *Lman1*$^{gt1/gt1}$ mice, at ~60% of WT levels (Figure 2A), and are significantly higher than for *Mcfd2*$^{-/-}$ mice ($P < .0001$ for FV and FVIII). In vitro studies by Nyfeler et al suggest that AAT is also an LMAN1 cargo.[20] However, plasma AAT levels are not significantly decreased in LMAN1-KO mice, as determined by western blot analysis.[17] We analyzed plasma AAT levels using a more quantitative ELISA method. Plasma AAT levels were higher in male mice than in female mice, consistent with previous reports.[30] We observed small, but statistically significant, decreases in AAT levels in male mice of all 3 KO mouse lines ($P < .05$) but not in female mice (Figure 2B).

FV and AAT accumulate in the ER of LMAN1- and MCFD2-deficient mice

Intracellular FVIII expression in vivo is too low to be detected by currently available methods. Therefore, we focused our analysis on FV, reasoning that functions of LMAN1 and MCFD2 should be similarly reflected in FV and FVIII. Using an antibody that detects intracellular FV by western blot analysis, we found elevated FV levels in liver of all 3 KO mouse lines compared with WT mice (Figure 3A), consistent with a defect in ER exit. Similar to LMAN1-KO mice, higher intracellular levels of AAT were also observed in MCFD2-KO and DKO mice (Figure 3). Intracellular AAT was increased in livers of all 3 KO mouse lines in male and female mice, with higher levels observed in males (Figure 3B), consistent with the higher plasma AAT levels detected in male mice. To distinguish between proteins accumulating in the ER and proteins that have moved into the Golgi and beyond, we treated liver extracts with endoglycosidase H (endo H), which cleaves high-mannose oligosaccharides from *N*-linked glycoproteins in the ER

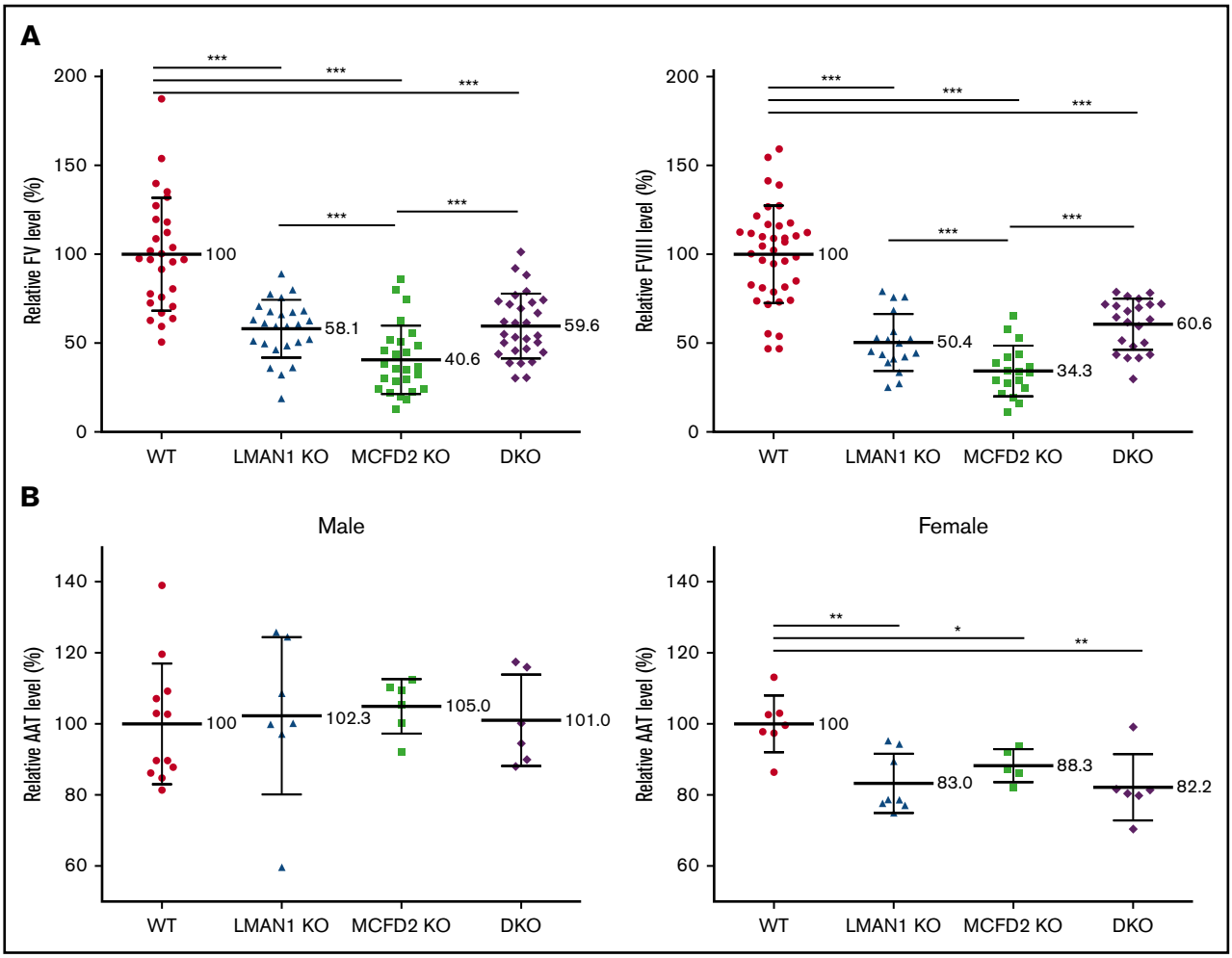

Figure 2. FV, FVIII, and AAT levels in WT, *Lman1*$^{gt1/gt1}$, *Mcfd2*$^{-/-}$, and DKO mice. (A) Plasma was collected from blood drawn by cardiac puncture from mice euthanized at ~6 months of age. FV antigen and FVIII activity levels in 3 deficient mice were normalized against average WT levels. (B) Plasma AAT levels were measured by ELISA, and comparisons were made within male and female groups of mice. Error bars indicate SD. *$P < .05$, **$P <. 01$, ***$P < .001$.

and the cis Golgi. Glycoproteins that have moved into the medial Golgi are resistant to endo H. FV bands shifted to faster migration positions in sodium dodecyl sulfate-polyacrylamide gel electrophoresis after endo H treatment, consistent with the removal of *N*-linked glycans, indicating that the majority of intracellular FV is located in the ER (Figure 4A). Thus, higher FV levels in MCFD2 and DKO liver cell extracts represent increased FV protein retained in the ER.

Intracellular AAT was detected as 2 bands by immunoblotting (Figure 3). The upper band of AAT migrates at the same position as plasma AAT (Figure 3B) and is resistant to endo H treatment (Figure 4A), therefore corresponding to a postmedial Golgi fraction of the protein. The lower band of AAT is sensitive to endo H treatment, indicating that this is the ER species (Figure 4A). The intensity of the lower band increased in all 3 KO mouse lines, suggesting that AAT accumulates in the ER of hepatocytes of these mice (Figure 3A). Consistent with the immunoblotting results, immunofluorescence staining of frozen liver sections demonstrated increased intracellular accumulation of AAT in hepatocytes of all 3 KO mouse lines (Figure 4B).

Discussion

Similar to LMAN1 deficiency,[17] MCFD2 deficiency in mice leads to less marked reductions in plasma FV and FVIII levels than in human F5F8D patients with MCFD2 mutations.[16] FV and FVIII levels are lower in MCFD2-KO mice compared with the previously reported LMAN1-KO mice,[17] which are consistent with observations in humans with mutations in the *MCFD2* versus *LMAN1* genes.[16] Murine FV is produced in hepatocytes and megakaryocytes,[24,29] whereas FVIII is synthesized in endothelial cells.[18,31] In addition, FV protein levels are nearly 2 orders of magnitude higher than those of FVIII.[32] Thus, the LMAN1–MCFD2 cargo receptor must function in different cell types and transport proteins of vastly different abundances. MCFD2 deficiency has no effect on LMAN1 level, and a small amount of MCFD2 exists in LMAN1-deficient cells.[5] LMAN1 and MCFD2 have been shown to interact with FVIII independently of each other,[11,12] raising the possibility that deficiency of either protein alone may not completely abolish cargo receptor function. However, ablation of both components of the LMAN1–MCFD2 cargo receptor did not further reduce FV and FVIII levels, suggesting that an alternative secretory pathway may be

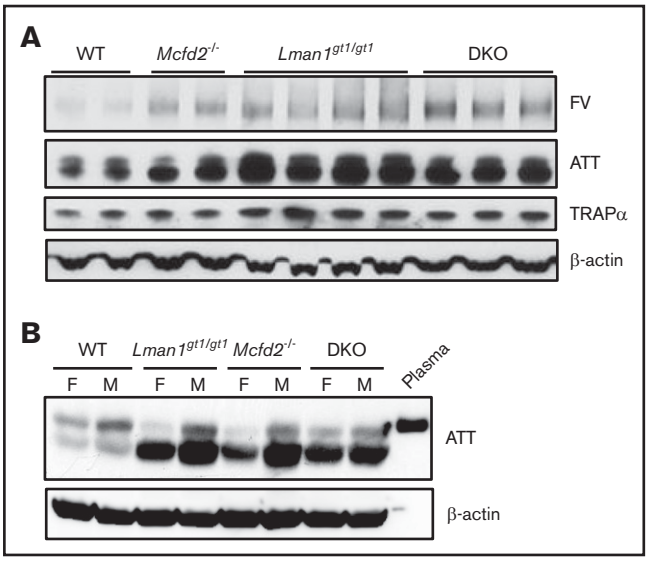

Figure 3. Intracellular FV and AAT levels in WT, *Lman1*$^{gt1/gt1}$, *Mcfd2*$^{-/-}$, and DKO mice. (A) Comparison of liver FV and AAT levels. Equal amounts of cell lysates (20 μg) from male mouse liver of the indicated genotypes were immunoblotted for FV, AAT, and TRAPα, an ER-resident protein. (B) Comparison of liver AAT levels in male and female mice. Equal amounts of cell lysates (20 μg) from mouse liver of the indicated genotypes and genders were immunoblotted for AAT and β-actin. A WT plasma sample was loaded in the last lane as a positive control.

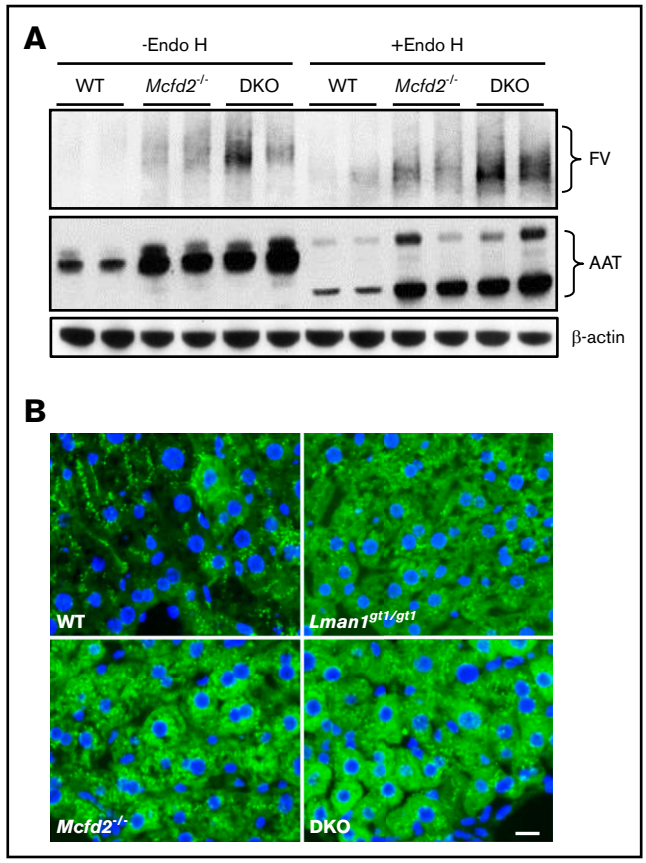

Figure 4. Endo H sensitivity of intracellular FV and AAT in WT, *Lman1*$^{gt1/gt1}$, *Mcfd2*$^{-/-}$, and DKO mice. (A) Liver lysates of male WT, *Mcfd2*$^{-/-}$, and DKO mice were treated or not with endo H and analyzed by immunoblotting with anti-FV, anti-AAT, and anti–β-actin antibodies. (B) Immunofluorescence staining of frozen sections of WT, *Lman1*$^{gt1/gt1}$, *Mcfd2*$^{-/-}$, and DKO liver for AAT. Identical staining protocols were performed simultaneously for all samples. Scale bar, 25 μm.

responsible for residual FV/FVIII secretion in DKO mice. Surprisingly, FV and FVIII in DKO mice match the higher levels found in LMAN1-KO mice and not the lower levels of MCFD2 mice. Mechanisms that might explain this puzzling observation include a compensatory increase in an alternative FV/FVIII-secretion pathway (potentially mediated by an alternative cargo receptor) in the absence of LMAN1, but not MCFD2, although few ER-to-Golgi cargo receptors have been identified in mammalian cells.[33-36] Previous immunoprecipitation studies, with and without a chemical cross-linker, were unable to identify any other interaction partners for LMAN1 or MCFD2.[5,10-12]

LMAN1 and MCFD2 are both widely expressed, including in many cell types that do not express FV and FVIII,[17] suggesting functions in addition to FV and FVIII transport. In vitro studies suggest that MCFD2 may function as an autocrine/paracrine factor for the maintenance of neural stem cells.[37,38] However, the lack of neurological and cognitive manifestations in F5F8D patients and mice argues against an essential role in neural stem cell survival in vivo. In contrast to the partial lethality observed in C57BL/6J LMAN1-KO mice, MCFD2-KO mice exhibit normal survival. These data suggest the existence of an additional cargo(s) that is dependent on LMAN1 but not MCFD2. The LMAN1-KO partial lethal phenotype is unlikely to be due to bleeding, given the only modest reductions in FV and FVIII levels. These data suggest a requirement in late embryogenesis for another, as yet unknown, LMAN1 cargo(s), with variable levels of expression for this cargo, or another component of the associated pathway, across mouse strains.

Although the ER-to-Golgi transport of FV and FVIII requires LMAN1 and MCFD2, previous reports suggest that MCFD2 is dispensable for certain cargo proteins, such as the lysosomal enzymes cathepsin C and cathepsin Z in vitro,[39] although no decrease in steady-state levels of cathepsin Z was detected in plasma of *Lman1*$^{gt1/gt1}$ mice.[17] However, we observed AAT accumulation in the ER of liver hepatocytes in single-KO and DKO mice, suggesting that LMAN1 and MCFD2 are also required for ER-to-Golgi transport of AAT. ER accumulation of AAT, although similar to that of FV, is only accompanied by a slight reduction in plasma AAT levels in male mice, suggesting that the steady-state AAT level in plasma is subject to additional regulation. Residual secretion of AAT and FV/FVIII in DKO cells suggests the existence of an alternative ER-to-Golgi transport pathway for this glycoprotein, as well as for FV/FVIII. The mechanism responsible for a mild decrease in plasma AAT only in male mice is unknown, although AAT levels are upregulated by testosterone and downregulated by estradiol,[30] suggesting the potential for a slight shift in the balance of AAT synthesis and degradation in male vs female mice. Taken together, our studies suggest additional nonoverlapping functions of LMAN1 and MCFD2 in vivo.

Acknowledgments

The authors thank Bilge Ozel for assistance with statistical analysis.

This study was supported by grants from the National Institutes of Health, National Heart, Lung, and Blood Institute (R01HL094505 and R35HL135793) (D.G.) and National Cancer Institute (R03CA202131) (B.Z.) and the Natural Science Foundation of Xinjiang Uygur Autonomous Region (2016D01A020 [M.Z.]). D.G is an investigator at the Howard Hughes Medical Institute.

Authorship

Contribution: B.Z., C.Z., M.Z., and D.G. designed the study; C.Z., M.Z., L.E., W.W., and B.Z. performed research; C.Z., M.Z., and B.Z. analyzed data and wrote the manuscript; and all authors provided critical comments.

Conflict-of-interest disclosure: The authors declare no competing financial interests.

ORCID profile: B.Z., 0000-0002-7786-7580.

Correspondence: Bin Zhang, Genomic Medicine Institute, Lerner Research Institute of Cleveland Clinic, 9500 Euclid Ave/NE50, Cleveland, OH 44195; e-mail: zhangb@ccf.org.

References

1. Kaufman RJ, Fay PJ, Popolo L, Ortel TL. Factor V and factor VIII. In: Marder VJ, Aird WC, Bennet JS, Schulman S, White GC, eds. *Hemostasis and Thrombosis: Basic Principles and Clinical Practice*. Philadelphia, PA: Lippincott William & Wilkins; 2013:179-196.
2. Seligsohn U, Zivelin A, Zwang E. Combined factor V and factor VIII deficiency among non-Ashkenazi Jews. *N Engl J Med*. 1982;307(19):1191-1195.
3. Zheng C, Zhang B. Combined deficiency of coagulation factors V and VIII: an update. *Semin Thromb Hemost*. 2013;39(6):613-620.
4. Nichols WC, Seligsohn U, Zivelin A, et al. Mutations in the ER-Golgi intermediate compartment protein ERGIC-53 cause combined deficiency of coagulation factors V and VIII. *Cell*. 1998;93(1):61-70.
5. Zhang B, Cunningham MA, Nichols WC, et al. Bleeding due to disruption of a cargo-specific ER-to-Golgi transport complex. *Nat Genet*. 2003;34(2):220-225.
6. Itin C, Roche AC, Monsigny M, Hauri HP. ERGIC-53 is a functional mannose-selective and calcium-dependent human homologue of leguminous lectins. *Mol Biol Cell*. 1996;7(3):483-493.
7. Kappeler F, Klopfenstein DR, Foguet M, Paccaud JP, Hauri HP. The recycling of ERGIC-53 in the early secretory pathway. ERGIC-53 carries a cytosolic endoplasmic reticulum-exit determinant interacting with COPII. *J Biol Chem*. 1997;272(50):31801-31808.
8. Nufer O, Kappeler F, Guldbrandsen S, Hauri HP. ER export of ERGIC-53 is controlled by cooperation of targeting determinants in all three of its domains. *J Cell Sci*. 2003;116(Pt 21):4429-4440.
9. Guy JE, Wigren E, Svärd M, Härd T, Lindqvist Y. New insights into multiple coagulation factor deficiency from the solution structure of human MCFD2. *J Mol Biol*. 2008;381(4):941-955.
10. Zheng C, Liu HH, Zhou J, Zhang B. EF-hand domains of MCFD2 mediate interactions with both LMAN1 and coagulation factor V or VIII. *Blood*. 2010;115(5):1081-1087.
11. Zhang B, Kaufman RJ, Ginsburg D. LMAN1 and MCFD2 form a cargo receptor complex and interact with coagulation factor VIII in the early secretory pathway. *J Biol Chem*. 2005;280(27):25881-25886.
12. Zheng C, Liu HH, Yuan S, Zhou J, Zhang B. Molecular basis of LMAN1 in coordinating LMAN1-MCFD2 cargo receptor formation and ER-to-Golgi transport of FV/FVIII. *Blood*. 2010;116(25):5698-5706.
13. Baines AC, Zhang B. Receptor-mediated protein transport in the early secretory pathway. *Trends Biochem Sci*. 2007;32(8):381-388.
14. Barlowe C, Helenius A. Cargo capture and bulk flow in the early secretory pathway. *Annu Rev Cell Dev Biol*. 2016;32(1):197-222.
15. Zheng C, Page RC, Das V, et al. Structural characterization of carbohydrate binding by LMAN1 protein provides new insight into the endoplasmic reticulum export of factors V (FV) and VIII (FVIII). *J Biol Chem*. 2013;288(28):20499-20509.
16. Zhang B, Spreafico M, Zheng C, et al. Genotype-phenotype correlation in combined deficiency of factor V and factor VIII. *Blood*. 2008;111(12):5592-5600.
17. Zhang B, Zheng C, Zhu M, et al. Mice deficient in LMAN1 exhibit FV and FVIII deficiencies and liver accumulation of α1-antitrypsin. *Blood*. 2011;118(12):3384-3391.
18. Everett LA, Cleuren AC, Khoriaty RN, Ginsburg D. Murine coagulation factor VIII is synthesized in endothelial cells. *Blood*. 2014;123(24):3697-3705.
19. Janciauskiene SM, Bals R, Koczulla R, Vogelmeier C, Köhnlein T, Welte T. The discovery of α1-antitrypsin and its role in health and disease. *Respir Med*. 2011;105(8):1129-1139.
20. Nyfeler B, Reiterer V, Wendeler MW, et al. Identification of ERGIC-53 as an intracellular transport receptor of alpha1-antitrypsin. *J Cell Biol*. 2008;180(4):705-712.
21. Motto DG, Chauhan AK, Zhu G, et al. Shigatoxin triggers thrombotic thrombocytopenic purpura in genetically susceptible ADAMTS13-deficient mice. *J Clin Invest*. 2005;115(10):2752-2761.
22. Soliman GA, Ishida-Takahashi R, Gong Y, et al. A simple qPCR-based method to detect correct insertion of homologous targeting vectors in murine ES cells. *Transgenic Res*. 2007;16(5):665-670.
23. Yang TL, Cui J, Rehumtulla A, et al. The structure and function of murine factor V and its inactivation by protein C. *Blood*. 1998;91(12):4593-4599.
24. Yang TL, Pipe SW, Yang A, Ginsburg D. Biosynthetic origin and functional significance of murine platelet factor V. *Blood*. 2003;102(8):2851-2855.

25. Doering C, Parker ET, Healey JF, Craddock HN, Barrow RT, Lollar P. Expression and characterization of recombinant murine factor VIII. *Thromb Haemost*. 2002;88(3):450-458.

26. Tao J, Zhu M, Wang H, et al. SEC23B is required for the maintenance of murine professional secretory tissues. *Proc Natl Acad Sci USA*. 2012;109(29): E2001-E2009.

27. Zhu M, Tao J, Vasievich MP, et al. Neural tube opening and abnormal extraembryonic membrane development in SEC23A deficient mice. *Sci Rep*. 2015; 5(1):15471.

28. Broze GJ Jr, Yin ZF, Lasky N. A tail vein bleeding time model and delayed bleeding in hemophiliac mice. *Thromb Haemost*. 2001;85(4):747-748.

29. Sun H, Yang TL, Yang A, Wang X, Ginsburg D. The murine platelet and plasma factor V pools are biosynthetically distinct and sufficient for minimal hemostasis. *Blood*. 2003;102(8):2856-2861.

30. Yamamoto K, Sinohara H. Regulation by sex hormones of serum levels of contrapsin and alpha 1-antiprotease in the mouse. *Biochim Biophys Acta*. 1984;798(2):231-234.

31. Fahs SA, Hille MT, Shi Q, Weiler H, Montgomery RR. A conditional knockout mouse model reveals endothelial cells as the principal and possibly exclusive source of plasma factor VIII. *Blood*. 2014;123(24):3706-3713.

32. Lynch CM, Israel DI, Kaufman RJ, Miller AD. Sequences in the coding region of clotting factor VIII act as dominant inhibitors of RNA accumulation and protein production. *Hum Gene Ther*. 1993;4(3):259-272.

33. Ladasky JJ, Boyle S, Seth M, et al. Bap31 enhances the endoplasmic reticulum export and quality control of human class I MHC molecules. *J Immunol*. 2006;177(9):6172-6181.

34. Mitrovic S, Ben-Tekaya H, Koegler E, Gruenberg J, Hauri HP. The cargo receptors Surf4, endoplasmic reticulum-Golgi intermediate compartment (ERGIC)-53, and p25 are required to maintain the architecture of ERGIC and Golgi. *Mol Biol Cell*. 2008;19(5):1976-1990.

35. Saito K, Chen M, Bard F, et al. TANGO1 facilitates cargo loading at endoplasmic reticulum exit sites. *Cell*. 2009;136(5):891-902.

36. Saito K, Yamashiro K, Ichikawa Y, et al. cTAGE5 mediates collagen secretion through interaction with TANGO1 at endoplasmic reticulum exit sites. *Mol Biol Cell*. 2011;22(13):2301-2308.

37. Liu H, Zhao B, Chen Y, et al. Multiple coagulation factor deficiency protein 2 contains the ability to support stem cell self-renewal. *FASEB J*. 2013;27(8): 3298-3305.

38. Toda H, Tsuji M, Nakano I, et al. Stem cell-derived neural stem/progenitor cell supporting factor is an autocrine/paracrine survival factor for adult neural stem/progenitor cells. *J Biol Chem*. 2003;278(37):35491-35500.

39. Nyfeler B, Zhang B, Ginsburg D, Kaufman RJ, Hauri HP. Cargo selectivity of the ERGIC-53/MCFD2 transport receptor complex. *Traffic*. 2006;7(11): 1473-1481.